# *Thermal Properties of Silica Aerogel Formula*



**Citation:** Cohen, Ellann, and Leon Glicksman. "Thermal Properties of Silica Aerogel Formula." Journal of Heat Transfer 137.8 (2015): 81601.

**As Published:** http://dx.doi.org/10.1115/1.4028901

**Publisher:** American Society of Mechanical Engineers (ASME)

**Persistent URL:** http://hdl.handle.net/1721.1/106629

**Version:** Final published version: final published article, as it appeared in a journal, conference proceedings, or other formally published context

# Thermal Properties of Silica Aerogel Formula

**Ellann Cohen**
Building Technology Program,
Department of Architecture and
Department of Mechanical Engineering,
Massachusetts Institute of Technology,
Cambridge, MA 02139
e-mail: ellann@alum.mit.edu

**Leon Glicksman**
Building Technology Program,
Department of Architecture and
Department of Mechanical Engineering,
Massachusetts Institute of Technology,
Cambridge, MA 02139
e-mail: glicks@mit.edu

*The thermal conductivity of silica aerogel developed in this research program was measured using the transient hot-wire technique. The thermal conductivity of monolithic samples drops significantly from 9.3 mW/m·K to 3.2 mW/m·K with modest pressure reduction from 1 atm to 0.1 atm. The same aerogel in granular form has a thermal conductivity of 15.0 mW/m·K at ambient gas pressure with a modest compression applied to compact the granules and reduce the air void sizes. Radiation heat transfer in the hot-wire test may not be representative of its contribution in large scale applications. Measurements of the monochromatic extinction coefficient over the wavelengths of interest resulted in a Rosseland mean extinction coefficient of 2400 $m^{-1}$ at 300 K. The small thermal penetration distance during the hot-wire measurements suggest that in actual use radiation could contribute approximately 2.5 mW/m·K with a possible upper limit of 3.0 mW/m·K to the effective thermal conductivity over that measured using the transient hot-wire method.* [DOI: 10.1115/1.4028901]

*Keywords: aerogel, thermal conductivity, radiation, hot-wire measurement*

## Introduction

Many governments, organizations, and companies are setting very ambitious goals to reduce their energy use over the next few years. Because the time periods for these goals are much less than the average lifetime of a building, existing buildings will need to be retrofitted. One of the most effective ways to improve building energy efficiency is to increase the insulation value of the envelope. Thin insulation panels can accomplish this while minimizing the impact on interior space. Aerogels are amongst the lowest conductivity insulation materials and will likely be a promising insulation for the future [1,2]. As part of a research program to develop advanced insulation panels, a number of small aerogel samples have been produced with different formulations. Using a transient hot-wire technique, the thermal conductivity of the samples was measured at atmospheric and reduced pressures. Extinction coefficients in the infrared regime were also obtained to determine possible corrections for radiative effects.

Aerogel thermal properties can vary widely depending on the production method, the formula used to create it, and the base component. The aerogels with the lowest thermal conductivities are those made from silica. Figure 1 shows the thermal conductivities reported by Caps and Fricke [3], Heinemann et al. [4], Lee et al. [5], Rigacci and Tantot-Neirac [6], Zeng et al. [7], and Wei et al. [8]. There are three important things to note from this data. First, the thermal conductivity of silica aerogels decreases with reduced pressure. Second, when comparing the monolithic samples to the granular sample, there is a significant difference in the shape of the curve representing the thermal conductivity variation with pressure. This different behavior can be explained by comparing the gas cavity widths in the granular sample to the pore sizes in the monolithic aerogel. The gas conductivity begins to decrease as the gas mean free path approaches the characteristic dimension of the void or cavity it is contained in. The pores that contain gas in the aerogel structure are very small (on the order of 2–100 nm), which is already on the same order of magnitude as the gas mean free path length. By reducing the pressure, the gas mean free path length increases. Once the gas mean free path is limited by the pore size, the thermal conductivity starts to drop. In the granular sample, there are relatively large voids or gas cavities between the granules, which are much larger than the ambient gas mean free path. Thus the pressure has to be reduced considerably before the gas mean free path increases to the same order of magnitude as the cavity widths and the thermal conductivity begins to decrease significantly. Models of the influence of air pressure on conductivity have been proposed by Wei et al. [9] and Zeng et al. [10]. A modest pressure reduction of monolithic aerogel, e.g., 0.1 atm, can lead to substantial reduction of conductivity as can be seen in Fig. 1. This reduces the requirement for high performance envelopes to maintain the properties over a long life. Several authors have shown that the conductivity can be decreased further by the addition of carbon to reduce the contribution of radiation, Zeng et al. [11].

In this paper, the thermal properties for a new improved recipe for silica aerogel are presented. This includes a comparison of the monolithic versus granular samples since these performance differences could be significant to the application of new insulations. A few other aerogels were measured as well in order to verify the validity of our results.

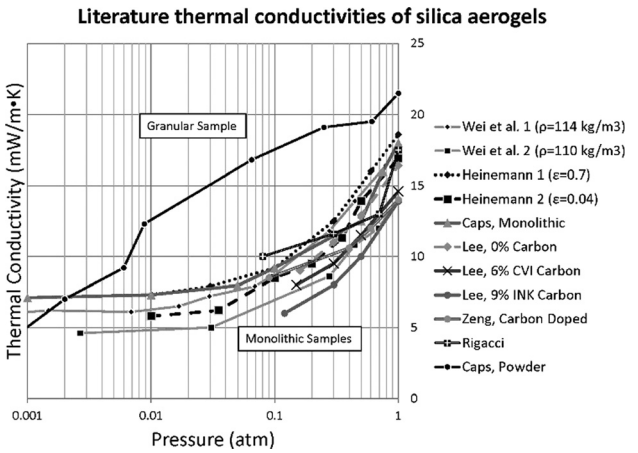


**Fig. 1 Survey of literature silica aerogel thermal conductivities across pressure**

Contributed by the Heat Transfer Division of ASME for publication in the Journal of Heat Transfer. Manuscript received June 28, 2013; final manuscript received October 3, 2014; published online April 21, 2015. Assoc. Editor: Patrick E. Phelan.

  

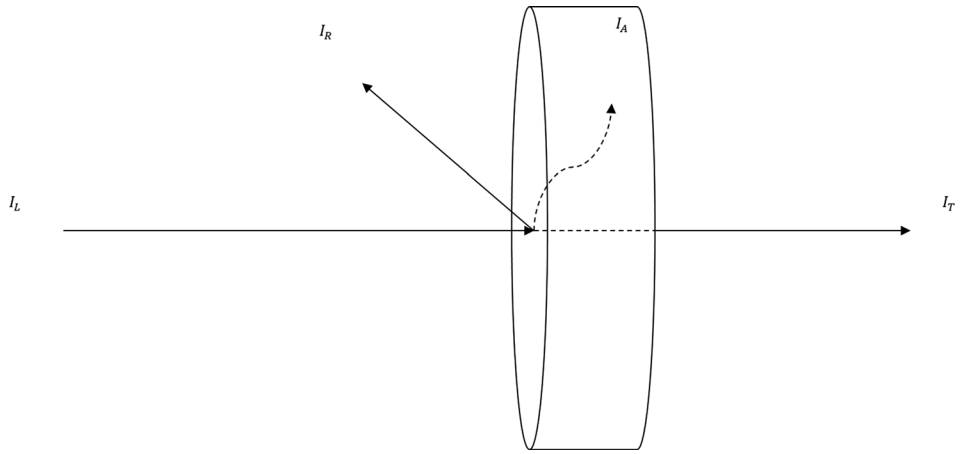


**Fig. 2 Various radiation intensities during an FTIR test**

## Experimental Setup

The primary method used to measure thermal conductivity in this study is the transient hot-wire method. This method involves embedding a thin wire with a known temperature—electrical resistance relationship into the aerogel and running a specified current through the wire for a specified duration. The slope of the temperature rise over ln(time) relates directly to the thermal conductivity of the aerogel. Because the aerogel has such a low thermal conductivity and because the thin platinum hot-wire is soldered at either end to a much-thicker copper wire (which has very low thermal resistance), the hot-wire is much cooler at the ends than in the middle. The experimental measurements are used to obtain the average temperature of the hot-wire, which will result in an overestimate of the thermal conductivity in this setup. To correct for these end effects, we modeled the temperature distribution along the wire based on the average temperature measured, found the temperature of the middle of the wire, and then used this value to calculate the actual thermal conductivity of the aerogel. This correction was validated to within 1 mW/m · K for NIST standard reference material 1459 ($k = 20.6$ mW/m · K); therefore, removing the dependency on hot-wire length from the thermal conductivity measurements (Cohen and Glicksman [12]).

## Radiation

For semitransparent materials like aerogels, the energy from the hot-wire is transferred by a combination of conductive and radiative heat transfer. The radiative component might not be taken into account properly by means of a short transient test using a fine radial wire such as the hot-wire test. In thick insulation under steady state conditions, the radiation heat transfer through the cellular solid insulation may be more significant. In addition, radiation effects will differ if the mean free path of radiation is an order of magnitude smaller than the penetration of the thermal transient into the test material or, on the other hand, if the mean free path of the radiation is larger than the test sample. Therefore, we performed Fourier transform infrared spectroscopy (FTIR) tests on our aerogel to measure the transmissivity. From these measurements we calculated the mean free path of radiation, the extinction coefficient, and the potential addition of radiation to the effective thermal conductivity measured by the transient hot-wire method. Note that this same issue may be critical when using a very short time transient planar source technique for measuring thermal conductivity.

**FTIR for Transmissivity, Extinction Coefficient, and Optical Thickness.** FTIR was used to measure the transmissivity ($\tau_\lambda$) of an aerogel sample at different wavelengths. $\tau_\lambda$ is defined as the ratio of intensity of the collimated radiation created by a laser that is transmitted through a material ($I_T$) at a single wavelength ($\lambda$) to the intensity of radiation that initially enters the material ($I_0$) at the same wavelength as shown in the equation below:

$$\tau_\lambda = \frac{I_T}{I_0} \tag{1}$$

The FTIR machine measures the ratio of the intensity of radiation that passes through the material ($I_T$) to the intensity of radiation emitted from the laser ($I_L$). $I_0$ differs from $I_L$ because a portion of the radiation from the laser is reflected at the sample surface. Figure 2 shows the different paths of the radiation from the laser beam ($I_L$) as it hits and passes through a material. First, at the surface of the material, a portion is reflected ($I_R$) and the rest enters the material ($I_0$), Eq. (2). Then, a portion of $I_0$ is absorbed by the material ($I_A$) while the remainder is transmitted through to the detector ($I_T$), Eq. (3):

$$I_0 = I_L - I_R \tag{2}$$

$$I_0 = I_A + I_T \tag{3}$$

In order to get the correct value for transmissivity ($\tau_\lambda$), we need to account for the reflectance off the front surface of the aerogel ($I_R$). The reflectance is only dependent on the front surface of the material, while the transmissivity is dependent on the thickness of the material. Several different thicknesses of aerogel were tested. The reflectance component would ideally stay constant while the transmissivity decreased with sample thickness. Using Beer's law, Eq. (4), the relationship between transmissivity and thickness can be obtained, where $x$ is the thickness of the sample and $K_\lambda$ is the monochromatic extinction coefficient, a property of the aerogel

$$\frac{I_T}{I_0} = \frac{I_T}{I_L - I_R} = e^{-K_\lambda x} \tag{4}$$

Rearranging Eq. (4) and combining with Eq. (2) yields

$$\frac{I_T}{I_L} = \frac{I_0}{I_L}\frac{I_T}{I_0} = \frac{I_0}{I_L}e^{-K_\lambda x} = \left(1 - \frac{I_R}{I_L}\right)e^{-K_\lambda x} \tag{5}$$

We were able to create thin samples of the monolithic aerogel down to a thickness of 0.1 mm. This should give better resolution then using ground aerogel. We tested four different thicknesses of aerogel (between 0.1 mm and 1 mm). Thus, we had four equations (each based on Eq. (5)) and only two unknowns, $I_R/I_L$ and $K_\lambda$. Note that $I_T/I_L$ is the output from the FTIR machine. Using the four equations, we solved for the best fit value of $I_R/I_L$ and $K_\lambda$ for each wavelength of the experiment. The correct transmissivity

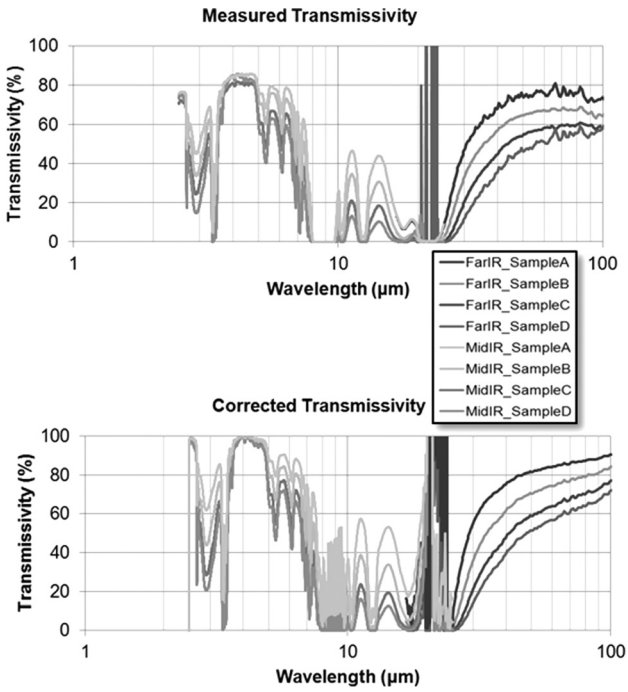


**Fig. 3 Measured transmissivity from FTIR machine of four sample thicknesses of MIT aerogel (16 E) and corrected transmissivity for the same samples (thicknesses: sample A—0.23 mm, sample B—0.39 mm, sample C—0.60 mm, and sample D—0.75 mm)**

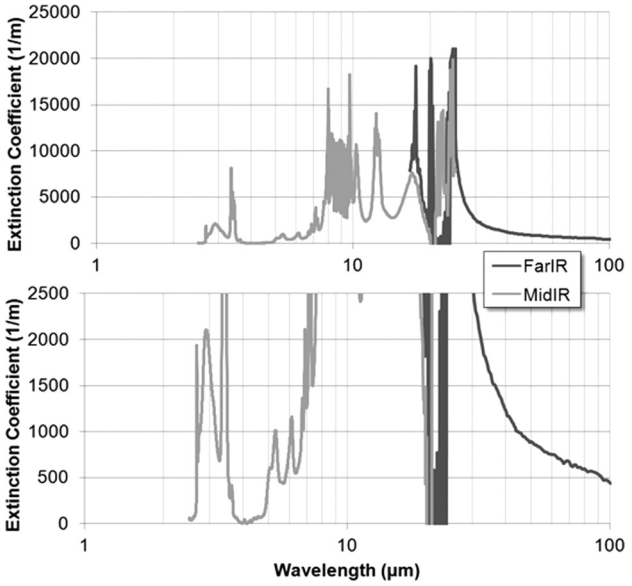


**Fig. 4 Extinction coefficient of MIT aerogel (16 E) at each wavelength in the mid to far infrared regions**

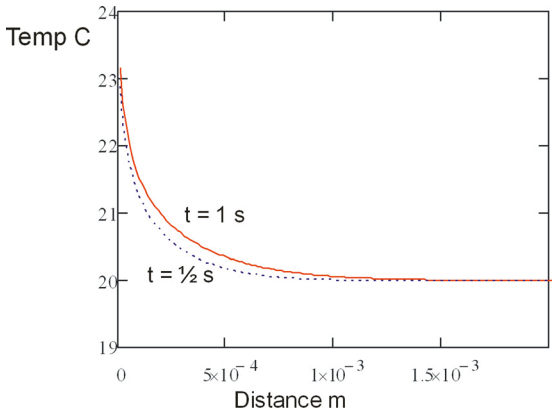


**Fig. 5 Predicted temperature distributions for transient tests, temperature versus distance from the wire surface (m)**

then can be determined from the best fit value of $K_\lambda$ for each wavelength. The measured value of $I_T/I_L$ of each sample and the correct transmissivity of each sample are shown in Fig. 3.

Note that the FTIR test had to split into two wavelength intervals for each sample—the far infrared wavelength range and the mid infrared wavelength range—because of the limits of the detectors in the machine.

The extinction coefficient for each wavelength $K_\lambda$ is calculated using the corrected transmissivity for each wavelength ($\tau_\lambda$) as well as the thickness of the sample ($x$) in Eq. (6).

$$K_\lambda = -\frac{\ln(\tau_\lambda)}{x} \tag{6}$$

The extinction coefficient calculated for each wavelength interval of one aerogel sample, identified as 16 E, is shown in Fig. 4.

From the extinction coefficients, one can determine the wavelengths for which the aerogel is optically thick, intermediate, or optically thin. Optical thickness ($t_{o_\lambda}$) is defined as

$$t_{o_\lambda} = K_\lambda x \tag{7}$$

where $x$ is the thickness of the material. A material is considered optically thick if $t_{o_\lambda} \gg 1$. For the sake of this paper, the aerogel will be considered optically thick if $t_{o_\lambda} \geq 5$; otherwise it will be considered intermediate optical thickness or optically thin.

Because of the small thickness of the aerogel samples, very short transient tests were used to limit the thermal penetration distance. A fine wire (25 $\mu$m in diameter) was used to insure that the Fourier number was much larger than unity. The analytical solution from Carslaw and Jaeger [13] for transient axisymmetric conduction from this wire with a constant heat source surrounded by aerogel with constant conductivity is shown in Fig. 5 for 0.5 s and 1 s.

Thus, for the transient hot-wire test, the thermal penetration depth is approximately 1.4 mm. For a wavelength interval to be considered optically thick the extinction coefficient must exceed $3500\,\mathrm{m}^{-1}$. Table 1 presents the wavelength intervals where the monochromatic extinction is less than $3500\,\mathrm{m}^{-1}$. This includes eight different wavelength regions, five of which in total account for approximately 43% of the blackbody energy. Note that in our hot-wire tests, 70% of the temperature increase occurs within a distance of about 0.1 mm–0.25 mm of the wire. If this value is thought of as the sample thickness, then a much higher percentage of radiation is in the intermediate or optically thin range.

The uncertainty dealing with the radiation in the hot-wire experiment is caused by the very small wire diameter and small thermal penetration distances. For such small bodies, radiation is minimized when compared to the relatively large magnitude of conduction. To illustrate, Eq. (8) compares the heat flux from the hot-wire ($q_{\mathrm{wire}}(t)$) to the maximum possible heat flux from radiation ($q_{\mathrm{rad}}(t)$) assuming that the hot-wire is a blackbody

$$\frac{q_{\mathrm{rad}}}{q_{\mathrm{wire}}}(t) = \frac{\mathrm{SA}_{\mathrm{wire}}\sigma(T_{\mathrm{wire}}(t)^4 - T_{\mathrm{amb}}^4)}{I^2R(t)} \tag{8}$$

where $\mathrm{SA}_{\mathrm{wire}}$ is the surface area of the hot-wire, $T_{\mathrm{wire}}(t)$ is the temperature of the hot-wire as a function of time, $T_{\mathrm{amb}}$ is the temperature of the surrounding material at the beginning of the test (or the temperature a long way from the hot-wire), $I$ is the current

**Table 1 Percent of blackbody energy in wavelength regions that are not optically thick for a material thickness of 1.4 mm**

| Wavelength regions ($\mu$m) with $k_\lambda < 3500\,m^{-1}$ | % Blackbody energy at 300 K |
|---|---|
| 2.499–3.335 | 0.03 |
| 3.372–3.389 | <0.01 |
| 3.418–3.432 | <0.01 |
| 3.459–7.648 | 11.85 |
| 10.781–11.758 | 6.29 |
| 13.365–15.118 | 8.71 |
| 18.653–19.790 | 3.18 |
| 28.340–199.440 | 12.54 |
| Total | 42.60 |

**Table 2 Percent of blackbody energy in wavelength regions that are not optically thick for a material thickness of 1 cm**

| Wavelength regions ($\mu$m) with $k_\lambda < 500\,m^{-1}$ | % Blackbody energy at 300 K |
|---|---|
| 2.499–2.666 | <0.01 |
| 3.523–5.000 | 1.23 |
| 5.499–5.813 | 0.92 |
| 94.280–199.440 | 0.56 |
| Total | 2.70 |

through the hot-wire, and $R(t)$ is the changing resistance of the hot-wire. An experiment was carried out using a blackened hot-wire. For the conditions of this test, the maximum ratio of radiation heat flux from the wire surface to the hot-wire's heat flux (Eq. (8)) is 5%. However, for this semitransparent media, emission and absorption from material at a radius of 0.1 mm could have a much larger influence on the overall heat flux since the surface area at this radius is an order of magnitude larger than the wire surface area. The challenge is to determine the wavelength intervals where the emission will be significant.

For large-scale planar samples, radiation is characterized by a diffusion approximation for the larger portion of the spectrum in the optically thick regime. This leads us to believe that radiation heat transfer in the hot-wire test may not be representative of its contribution in large scale applications. For larger diameter hot-wires, radiation may be more important and more closely characterize results for thick insulations.

For use in insulation, the aerogel will be much thicker, typically at least 1 cm. In this case, the aerogel will be optically thick in regions where the extinction coefficient is $500\,m^{-1}$. This includes most of the radiative spectrum for room temperature black body emission. The regions that are not optically thick are shown in Table 2 and account for only 2.7% of the total black body energy at room temperature.

**Rosseland Mean Extinction Coefficient.** When a material is optically thick, such as in a 1 cm thick insulation case, the net radiative heat flux is only dependent on local gradients of the emissive power. The radiation is emitted from one local point, absorbed at another and then re-emitted, absorbed, re-emitted, etc. This so called diffusion model is very similar to conduction. The net radiative heat flux for each wavelength ($q_\lambda$) can be described by the Rosseland diffusion equation below:

$$\frac{dq_\lambda}{d\lambda} = -\frac{4}{3K_{e_\lambda}}\frac{de_{b_\lambda}}{dx} \tag{9}$$

where $K_{e_\lambda}$ is the extinction coefficient of the material at each wavelength and $e_{b_\lambda}$ is the blackbody hemispherical flux at each wavelength [14]. Integrating this over all wavelengths in which the material is optically thick results in

$$\begin{aligned} q_{\Delta\lambda} &= \int_{\Delta\lambda} -\frac{4}{3K_{e_\lambda}}\frac{\partial e_{b_\lambda}}{\partial x}d\lambda \\ &\approx -\frac{4}{3K_{e_R,\Delta\lambda}}\frac{\partial e_b}{\partial x}\left[\frac{\int_{\Delta\lambda} e_{b_\lambda}d\lambda}{e_b}\right] \\ &\approx -\frac{4}{3K_{e_R,\Delta\lambda}}4\sigma T^3\frac{\partial T}{\partial x}\left[\frac{\int_{\Delta\lambda} e_{b_\lambda}d\lambda}{e_b}\right] \end{aligned} \tag{10}$$

where $q_{\Delta\lambda}$ is the net radiative heat flux over the wavelengths where the material is optically thick, $e_b$ is the total blackbody hemispherical flux over all wavelengths, $\int_{\Delta\lambda} e_{b_\lambda}d\lambda$ is the total blackbody hemispherical flux over all wavelengths in which the material is optically thick, $K_{e_R,\Delta\lambda}$ is defined as the Rosseland mean extinction coefficient (an extinction coefficient averaged over all wavelengths for which the material is optically thick and is described in more detail in the next paragraph), $\sigma$ is the Stefan–Boltzmann constant and $T$ is temperature. By relating this diffusion approximation to Fourier's law of conduction as shown below:

$$q_{\Delta\lambda} \approx -\frac{4}{3K_{e_R,\Delta\lambda}}4\sigma T^3\frac{\partial T}{\partial x}\left[\frac{\int_{\Delta\lambda} e_{b_\lambda}d\lambda}{e_b}\right] \approx k_{rad}\frac{dT}{dx} \tag{11}$$

one can determine an addition to the thermal conductivity due to radiation ($k_{rad}$) shown in Eq. (12). As explained above, this might not be accounted for in the data from the hot-wire method.

$$k_{rad} = \frac{16\sigma T^3}{3K_{e_R,\Delta\lambda}}\left[\frac{\int_{b_\lambda}^{e} d\lambda}{e_b}\right] \tag{12}$$

Now, we need to find the Rosseland mean extinction coefficient ($K_{e_R,\Delta\lambda}$) as defined by the equations below for regions where the material is optically thick:

$$\frac{1}{K_{e_R,\Delta\lambda}} = \frac{\int_{\Delta\lambda}\frac{1}{K_{e_\lambda}}\frac{\partial e_{b_\lambda}}{\partial x}d\lambda\frac{\partial x}{\partial T}}{\int_{\Delta\lambda}\frac{\partial e_{b_\lambda}}{\partial x}d\lambda\frac{\partial x}{\partial T}} = \frac{\int_{\Delta\lambda}\frac{1}{K_{e_\lambda}}\frac{\partial e_{b_\lambda}}{\partial T}d\lambda}{\int_{\Delta\lambda}\frac{\partial e_{b_\lambda}}{\partial T}d\lambda} \tag{13}$$

where $e_{b_\lambda}$ is the spectral hemispherical blackbody flux, $K_{e_\lambda}$ is the extinction coefficient at a specific wavelength, $T$ is the temperature (assumed to be 300 K), and $\lambda$ is the wavelength. Because the material is not optically thick across all wavelengths, the integrals in Eq. (13) cover only the optically thick wavelengths instead of wavelengths from zero to infinity. Also, since the extinction coefficient is not uniform across all of the optically thick regions, the integrals were broken up even further. The wavelength range of the data spans from 2.5 $\mu$m to 200 $\mu$m, the corresponding wave numbers were $4000\,cm^{-1}$ to $50\,cm^{-1}$. Because the mean extinction coefficient was calculated over narrow wavelength range intervals, corresponding to a wave number of $2\,cm^{-1}$, the Rosseland mean extinction coefficient equation in practice looks more like the following:

$$\frac{1}{K_{e_R,\Delta\lambda}} = \frac{\int_{\lambda_1}^{\lambda_2}\frac{1}{K_{e_\lambda}}\frac{\partial e_{b_\lambda}}{\partial T}d\lambda + \int_{\lambda_3}^{\lambda_4}\frac{1}{K_{e_\lambda}}\frac{\partial e_{b_\lambda}}{\partial T}d\lambda + \cdots}{\int_{\lambda_1}^{\lambda_2}\frac{\partial e_{b_\lambda}}{\partial T}d\lambda + \int_{\lambda_3}^{\lambda_4}\frac{\partial e_{b_\lambda}}{\partial T}d\lambda + \cdots} \tag{14}$$

where the Planck expression is used in the evaluation.

For the case of the hot-wire, where the material thickness is only 1.4 mm based on the penetration depth, the material is optically thick for only a small portion of the wavelengths and the resulting Rosseland mean extinction coefficient is $6300\,m^{-1}$, which results in an additional possible thermal conductivity of at most 0.75 mW/m · K. For the case of insulation with a thickness of 1 cm, the material is almost entirely optically thick. The resulting Rosseland mean extinction coefficient is $2400\,m^{-1}$, similar to the value obtained by Rettelbach et al. [15] of $3750\,m^{-1}$ for a denser granular sample at 300 K. Using our measured value which results in an additional possible thermal conductivity of 3.3 mW/m · K assuming there isn't any radiative augmentation to the conduction in our sample tests. However, our estimate suggest that there is a radiative contribution of 0.75 mW/m · K in our hot-wire tests This suggests that the correction to the measured conductivity values should be, as a first approximation, 2.5 mW/m · K with a possible upper limit of 3.3 mW/m · K when applied to thick insulation applications.

Note that this estimated contribution of radiation is of the same order as the improvements in effective conductivity found by Lee et al. [5] when they added carbon to their samples or Heinemann et al. [4] when the emissivity of the surfaces bounding their flat sample was decreased. For the present material, it is expected that similar means to reduce radiation influence could yield similar reductions. In that instance, the hot-wire measurement might be close to the final conductivity in larger panels with radiation abatement measures included.

**Blackened Hot-Wire.** To further test the effects of radiation in the aerogel, we performed two experiments on two samples of the same aerogel. One experiment used a polished hot-wire and the other used a blackened hot-wire. The latter was blackened with a VWR Chemical Resistant marker to limit any thickness addition to the diameter of the wire. The chemical resistance was necessary because during the processing of the gel to produce an aerogel, it is washed in ethanol, which dissolves most inks and paints. The wire was not perfectly coated when observed under a microscope, but it is estimated to have been coated by at least 75%. The results at various pressures for the samples with the polished wire and the blackened wire are shown in Fig. 6.

The results show that the emissivity of the wire does make a difference. The difference at ambient pressure is 1.1 mW/m · K, with a minimum difference of 0.2 mW/m · K at low pressure. It is expected that the emissivity at the wire surface influences the radiative transfer within one mean free path of the surface as well as the emission from the wire itself. Clearly this merits more detailed investigation.

**Previous Studies of Radiation in Transient Tests.** There have been studies by Gross and Tran [16] which have already looked at the interaction between radiation and an absorbing media as it influences thermal conductivity measurements made by the transient hot-wire method. They claim that the transient hot-wire technique is accurate for absorbing materials if the extinction coefficient exceeds $5000\,m^{-1}$ with temperatures near 25 °C.

But our hot-wire method is different from the past studies in several ways. First, the diameter of the hot-wire used by Gross and Tran was 500 $\mu$m, which is much larger than the 25 $\mu$m used in this study. The smaller diameter wire results in high values for the Fourier number (which can approach $10^{-3}$), which accurately simplifies the solution given by Carslaw and Jaeger. Similarly, for the short times that this test is run, there are very small penetration depths within the surrounding media. At one second into the test, 70% of the temperature change between the wire and the media is within 0.12 mm of the surface of the wire. Taking this dimension as $\delta$, the very small wire diameter results in conduction from the wire which is proportional to $k/\delta(\pi DL)$ (with very small $\delta$) which is substantially larger than radiation which is proportional to $h_r \pi DL$ where $h_r = 4\sigma T^3$. Second, aerogels are not gray bodies. In some wavelength regions, aerogels are very absorbing and act nearly opaque, while in other regions aerogels are very transparent and let radiation pass through with little interaction. With this wide range of transmissivity/absorption depending on the wavelength, it is not appropriate to assume one simple type of radiant heat transfer.

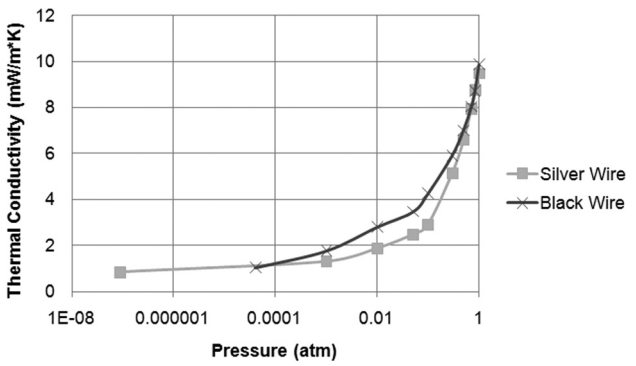


**Fig. 6 Thermal conductivity of aerogel (16 E) measured with two hot-wires: blackened (high emissivity) and silver-like/polished (low emissivity)**

## Thermal Conductivity Results

The results from the transient hot-wire method are presented below for several MIT recipes [17] of aerogel in granular and monolithic form as well as at reduced pressures. While the end effects are corrected for, no corrections have been applied to account for possible additional contributions from radiation. First, results from other aerogels are presented. These will then be compared to the results of the present study.

**Commercially Available Granules.** Granular aerogel from Cabot Corp. Cabot was tested using the transient hot-wire method. The granule thermal conductivity was measured by filling a container that had the hot-wire suspended in the middle with the granules and then compressing the granules around the wire to reduce any contact resistance between the wire and granules as well as to make the volume ratio of aerogel to air touching the wire as high as possible. The pressure applied was 10.4 kPa (1.5 psi). The reported thermal conductivity from Cabot Corp for their granules is 18 mW/m · K at ambient pressure. Our result, corrected for end effects, was 19.7 mW/m · K at the same pressure. This result is expected to vary as the compression is increased.

The thermal conductivity was also measured in a vacuum chamber over several pressures and the results are presented in Fig. 7 along with the literature results for monolithic aerogels and for powder. Notice that the granules follow a very different pattern than the monolithic aerogels. The monolithic aerogels have the greatest thermal conductivity decrease at moderate pressure levels while the granules have modest changes with initial pressure reduction; the greatest thermal conductivity decrease occurs at much lower pressures. This difference is consistent with other reported granule results from the literature such as Reim et al. [18].

**Cellulose Aerogel.** We have been focused on silica aerogel, but there are other aerogel possibilities as well. We obtained a sample of a cellulose based aerogel [19]. The sample had a density of $17.5\,kg/m^3$ as compared to $91\,kg/m^3$ for our silica aerogel. The thermal conductivity of a monolithic sample using the same hot-wire method as described previously yielded a conductivity of 28 mW/m · K, far in excess of approximately 10 mW/m · K for our silica aerogel.

Mechanical tests on the cellulose aerogel were performed as well and found a Young's modulus on the order of 200 kPa versus

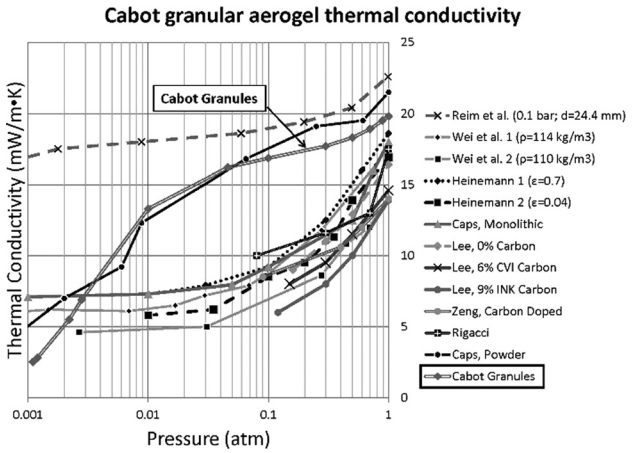


**Fig. 7 Thermal conductivities of aerogels across different pressures including Cabot Corp's granules**

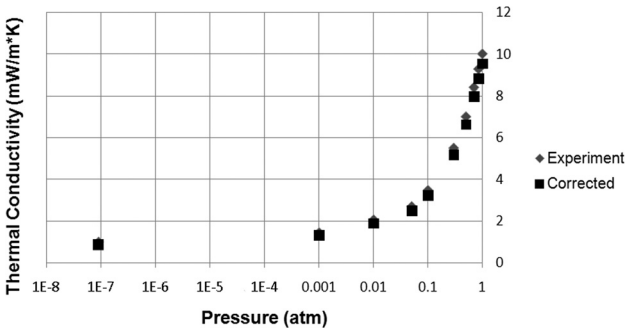


**Fig. 8 Thermal conductivity of our aerogel (16 E) at reduced pressures**

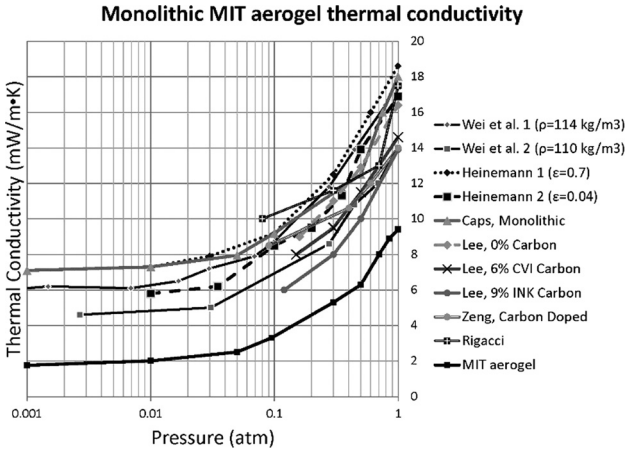


**Fig. 9 Thermal conductivity of our aerogel (16 E) compared to aerogels in the literature**

approximately 1 MPa for our silica aerogel. Using a scanning electron microscope, the pores in the cellulose aerogel were measured to be on the order of a few micrometers versus 2–100 nm for silica aerogel [20].This explains the higher thermal conductivity: the gas mean free path is significantly smaller than the pore width for the cellulose aerogel.

Both the thermal properties and the mechanical properties of the cellulose aerogel are not ideal for use as an advanced insulation.

**Monolithic MIT Aerogel at Reduced Pressure.** Previous studies by Caps and Fricke [3], Heinemann et al. [4], Lee et al. [5], Rigacci and Tantot-Neirac [6], Zeng et al. [7], and more suggest that with modest pressure reduction, monolithic aerogels have significantly reduced thermal conductivity. Caps, Heinemann, and Rigacci present results for pure silica aerogel, while Zeng and Lee present results for carbon-doped aerogels (the carbon included to help lower the radiation component of heat transfer). Heinemann used the guarded hot-plate method to measure the thermal conductivities and used boundaries with two different sets of emissivities. The trend across the different results is that the thermal conductivity drops the most dramatically as the pressure decreases from 1 atm to 0.1 atm for monolithic aerogel.

The MIT aerogel samples [17] were tested at several different gas pressures, mostly between 1 atm and 0.1 atm. The hot-wire method described previously was used in conjunction with a vacuum chamber and the end effects correction was applied. The results show the same approximate trends as expected from the literature for monolithic aerogels. The greatest reduction in thermal conductivity occurs between 1 atm and 0.1 atm. At higher vacuums (i.e., lower pressures), the thermal conductivity still decreases, but with diminishing returns. The results for the MIT aerogel are shown below in Fig. 8. Note that the end effects correction is more significant at the higher thermal conductivities.

Figure 9 shows the thermal conductivity versus pressure results for the various investigators along with the current aerogel results. As mentioned before, the general behavior of our results is similar yet the overall thermal conductivity is less than previous results at each pressure.

The improved performance in thermal conductivity could be explained by preliminary tests of void size that indicate finer cell sizes than that of aerogels made in previous investigations. Figure 10 shows a wider distribution of pore sizes along with smaller pores than observed by previous investigators. The reduction that is seen with reduced pressure only changes the gaseous conduction component of heat transfer. The results also suggest that it is definitely worth pursuing an insulation panel that is at reduced pressure, but only to 0.1 atm for monolithic samples.

**Granular Experimental Aerogel.** One concern with monolithic aerogels is that they are difficult to manufacture due to their fragility and long supercritical drying time. It is quicker and easier to manufacture granular aerogel. Using the same method described to measure the thermal conductivity of the Cabot granular samples, we measured the thermal conductivity of the experimental aerogel (16 E) in granular form, Fig. 11. The results are shown in Fig. 12. The maximum granule size was 5 mm in diameter with the majority being much smaller as shown in Fig. 11. The external compression pressure was up to 16.4 kPa (2.4 psi) which compressed the aerogel from a height of 12.7 mm–7.6 mm. The MIT granular samples were only tested at ambient air pressure.

**Comparing All Experimental Aerogel Recipes.** As part of the overall project, we were trying to develop a new silica aerogel recipe that would have reduced thermal conductivity with enhanced mechanical properties. Along the process, it was discovered that as the mechanical properties are improved the thermal conductivity unfortunately increases. Thus, the focus became to develop a recipe that has the lowest thermal conductivity possible yet maintains mechanical properties that enable handling. The thermal conductivity results for the main recipes tested are presented below. Note that the different aerogel recipes are differentiated by a number followed by letter "E". The number represents the solvent concentration as compared to silica—the higher the number, the higher the concentration. The E refers to the solvent being ethanol.

Three different methods of gelation were also used. In the one step method, hydrolysis, condensation, and gelation occur simultaneously after precursors and one catalyst are mixed. In the two step method, the precursors and a catalyst are mixed, causing hydrolysis. Then a different catalyst is added to induce condensation

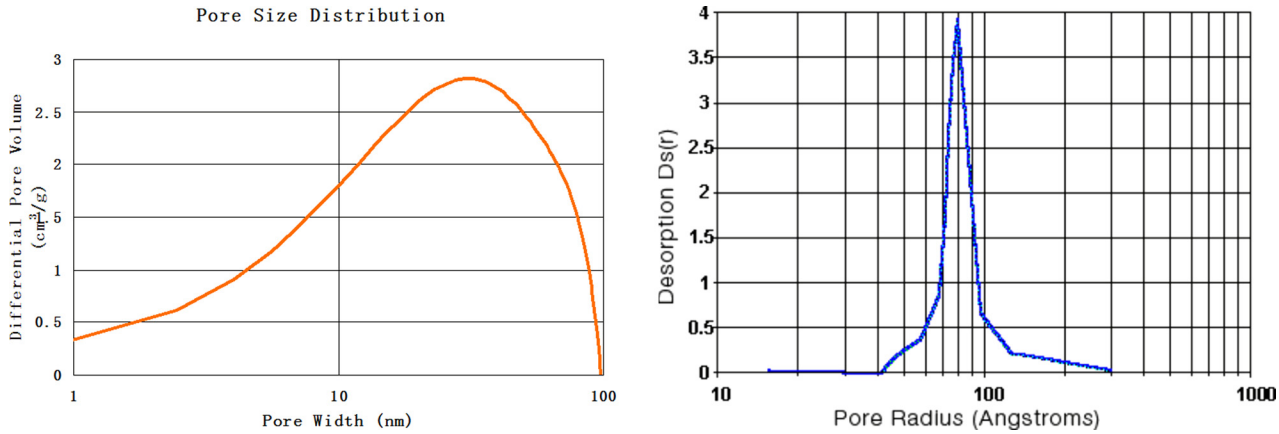


**Fig. 10 Pore size distribution current material [17], left, and previously reported [21], right**

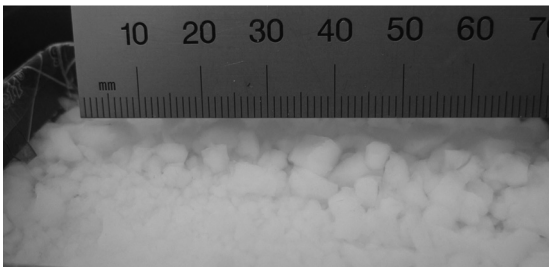


**Fig. 11 Granular aerogel (16 E) with ruler**

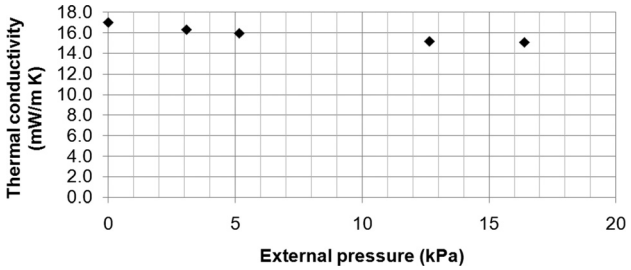


**Fig. 12 Thermal conductivity of granular aerogel (16 E) versus external pressure**

and gelation. In the three step method, there are three catalyst steps, which allows for better control over the aerogel's final pore size distribution. The only aerogels that were made using the one and two step methods are specifically labeled in the data presented below (i.e., 16 E-1step and 8 E-2step), while all the other aerogels were made using the three step method. The thermal conductivity of aerogel 16 E is presented both when measured by the silver-like polished surface hot-wire and blackened hot-wire. All other aerogels were measured using a polished hot-wire. All previously mentioned MIT aerogel sample results in this paper were 16 E measured with a silver wire and were made using the three step process.

Looking at Table 3 and Fig. 13, there is not a large difference in the thermal conductivities of the various monolithic MIT aerogel formulas. The 12 E sample starts out with the lowest thermal conductivity, but it is still within 0.6 mW/m · K of the 8 E-2step formula and the 16 E polished wire sample. By the time the pressure is reduced to 0.1 atm, the 16 E polished wire sample and the 16 E-1step samples have lower thermal conductivities. Since the idea for the final insulation is to use the aerogel at the slightly reduced pressure of 0.1 atm, it seems that the 16 E sample may be

**Table 3 Thermal conductivity comparison of all formula aerogels across pressures**

| | Thermal conductivity (mW/m·K) | | | | |
|---|---|---|---|---|---|
| Pressure (atm) | 16E Polished wire | 16E Black wire | 16E-1step | 12E | 8E-2step |
| 1.00 | 9.5 | 10.6 | 11.5 | 8.9 | 9.1 |
| 0.85 | 8.8 | 9.3 | 10.4 | 8.3 | 8.5 |
| 0.70 | 8.0 | 8.6 | 9.3 | 7.5 | 7.9 |
| 0.50 | 6.6 | 7.5 | 7.7 | 6.3 | 6.9 |
| 0.30 | 5.2 | 6.3 | 5.8 | 5.1 | 5.8 |
| 0.10 | 3.2 | 4.6 | 2.9 | 3.5 | 4.5 |
| 0.05 | 2.5 | 3.7 | 2.0 | 2.7 | 3.8 |
| 0.01 | 1.9 | 3.0 | 1.3 | 2.2 | 3.3 |
| 0.001 | 1.3 | 1.9 | 0.8 | 1.6 | 2.7 |
| <0.0001 | 0.86 | 1.1 | 0.4 | 1.1 | 2.1 |

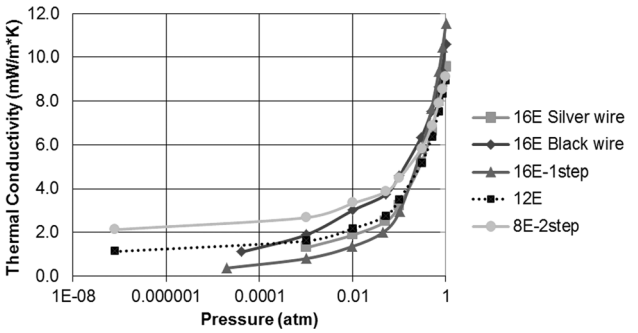


**Fig. 13 Thermal conductivity comparison of all formula aerogels across pressures. The standard silver-like/polished wire had a higher emissivity than the blackened wire.**

the best option. It has the second lowest thermal conductivity at 0.1 atm and still has a low thermal conductivity at 1 atm in case the slight vacuum is lost.

## Conclusion

The thermal conductivity of monolithic silica aerogel developed in this research program drops significantly from 9.3 mW/m · K to 3.2 mW/m · K with modest pressure reduction from 1 atm to 0.1 atm. The same aerogel in granular form has a thermal conductivity of 15.0 mW/m · K when at ambient gas pressure with a modest compression applied to compact the granules. Granular aerogel has to be reduced to a much lower gas pressure (and thus more expensive in a final product) to see reductions in thermal conductivity similar to the monolithic aerogel. On the other hand, granular aerogel should be cheaper to produce and can

more easily be inserted into an external structure. In future tests the granular aerogel will be subjected to different levels of compression.

Radiation may contribute up approximately 2.5 mW/m · K with an upper limit of 3.3 mW/m · K of additional thermal conductivity in large scale aerogel samples over that measured using the transient hot-wire method. In future research, larger aerogel samples should be tested in a guarded hot plate to verify the conductivity measurements.

## Acknowledgment

The research was funded by the DuPont-MIT Alliance. Dr. Vivek Kapur at DuPont and Mr. Adam Neugebauer of MIT contributed valuable insights. Professor Lars Berglund of KTH, Stockholm supplied the cellulose aerogel samples.

## Nomenclature

$e_b$ = total blackbody hemispherical flux over all wavelengths
$e_{b_\lambda}$ = monochromatic blackbody hemispherical flux
$I$ = current through the hot-wire
$I_A$ = intensity of light that is absorbed by the material
$I_L$ = intensity of light from the laser
$I_0$ = intensity of light that initially goes into the material
$I_R$ = intensity of light reflected off from surface of the material
$I_T$ = intensity of light that is transmitted through a material
$K_\lambda$ = monochromatic extinction coefficient
$K_{e_R,\Delta\lambda}$ = Rosseland mean extinction coefficient
$k_{rad}$ = thermal conductivity due to radiation
$q_\lambda$ = net radiative heat flux for each wavelength
$q_{\Delta\lambda}$ = net radiative heat flux over the wavelengths where the material is optically thick
$q_{rad}(t)$ = maximum possible heat flux from radiation
$q_{wire}(t)$ = heat flux from the hot-wire
$R(t)$ = the changing resistance of the hot-wire
$SA_{wire}$ = surface area of the hot-wire
$T$ = temperature
$t_{o_\lambda}$ = optical thickness
$T_{amb}$ = temperature of the surrounding material at the beginning of the test as well as the temperature a long way from the hot-wire
$T_{wire}(t)$ = temperature of the hot-wire as a function of time
$x$ = sample thickness
$\theta$ = temperature
$\lambda$ = wavelength
$\sigma$ = Stefan–Boltzmann constant
$\tau_\lambda$ = monochromatic transmissivity

## References

[1] Riffat, S., and Qiu, G., 2013, "A Review of State-of-Art Aerogel Applications in Buildings," Int. J. Low-Carbon Technol., **8**(1), pp. 1–6.
[2] Baetens, R., Bjorn, P., and Gustavsen, A., 2011, "Aerogel Insulation for Building Applications: A State–of-the-Art Review," Energy Build., **43**(4), pp. 761–769.
[3] Caps, R., and Fricke, J., 2004, "Aerogels for Thermal Insulation," *Sol-Gel Technologies for Glass Producers and Users*, M. A. Aegerter and M. Mennig, eds., Kluwer Academic, Boston, pp. 349–353.
[4] Heinemann, U., Caps, R., and Fricke, J., 1996, "Radiation-Conduction Interaction: An Investigation on Silica Aerogels," Int. J. Heat Mass Transfer, **39**(10), pp. 2115–2130.
[5] Lee, D., Stevens, P. C., Zeng, S. Q., and Hunt, A., 1995, "Thermal Characterization of Carbon-Opacified Silica Aerogels," J. Non-Cryst. Solids, **186**, pp. 285–290.
[6] Rigacci, A., and Tantot-Neirac, M., 2005, "Aerogel-Like Materials for Building Super-Insulation," 2nd International Symposium on Nanotechnology in Construction, Bilbao, Spain, Nov. 13–16, pp. 383–393.
[7] Zeng, S. Q., Hunt, A., and Greif, R., 1995, "Geometric Structure and Thermal Conductivity of Porous Medium Silica Aerogel," ASME J. Heat Transfer, **117**(4), pp. 1055–1058.
[8] Wei, G., Liu, Y., Zhang, X., Yu, F., and Du, X., 2011, "Thermal Conductivities Study of Silica Aerogel and Its Composite Insulation Materials," Int. J. Heat Mass Transfer, **54**(11–12), pp. 2355–2366.
[9] Wei, G., Liu, Y., Du, X., and Zhang, X., 2012, "Gaseous Conductivity Study on Silica Aerogel and Its Composite Insulation Materials," ASME J. Heat Transfer, **134**(4), p. 041301.
[10] Zeng, S., Hunt, A., Cao, W., and Grief, R., 1994, "Pore Size Distribution and Apparent Gas Thermal Conductivity of Silica Aerogel," ASME J. Heat Transfer, **116**(3), pp. 756–759.
[11] Zeng, S., Hunt, A., and Grief, R., 1995, "Theoretical Model of Carbon Content to Minimize Heat Transfer in Silica Aerogel," J. Non-Cryst. Solids, **186**, pp. 271–277.
[12] Cohen, E., and Glicksman, L., 2014, "Analysis of the Transient Hot-Wire Method to Measure Thermal Conductivity of Silica Aerogel: Influence of Wire Length, and Radiation Properties," ASME J. Heat Transfer, **136**(4), p. 04130.
[13] Carslaw, H. S., and Jaeger, J. C., 1959, *Conduction of Heat in Solids*, 2nd ed., Clarendon Press, Oxford, UK.
[14] Siegel, R., and Howell, J. R., 1981, *Thermal Radiation Heat Transfer*, 2nd ed., Hemisphere, Washington, DC.
[15] Rettelbach, T., Sauberlich, J., Korder, S., and Fricke, J., 1995, "Thermal Conductivity of Silica Aerogel Powders at Temperatures From 10 to 275 K," J. Non-Cryst. Solids, **186**, pp. 278–284.
[16] Gross, U., and Tran, L. T. S., 2004, "Radiation Effects on Transient Hot-Wire Measurements in Absorbing and Emitting Porous Media," Int. J. Heat Mass Transfer, **47**(14–16), pp. 3279–3290.
[17] Zuo, Y., 2010, "Preparation of Silica Aerogels With Improved Mechanical Properties and Extremely Low Thermal Conductivities Through Modified Sol-Gel Process," Master's thesis, Massachusetts Institute of Technology, Cambridge, MA.
[18] Reim, M., Reichenauer, G., Korner, W., Manara, J., Arduini-Schuster, M., Korder, S., Beck, A., and Fricke, J., 2004, "Silica-Aerogel Granulate—Structural, Optical, and Thermal Properties," J. Non-Cryst. Solids, **350**, pp. 358–363.
[19] Berglund, L., 2011, private communication.
[20] Goutierre, T., 2011, "Advanced Thermal Insulation for Energy Efficient Buildings: Structural Performance of Aerogel Composite Panels," Master's thesis, Massachusetts Institute of Technology, Cambridge, MA.
[21] Microstructured Materials Group at Lawrence Berkeley National Laboratory, pre-2004, "Science of Silica Aerogels: Physical Properties," Accessed Apr. 1, 2015, http://energy.lbl.gov/ecs/aerogels/sa-physical.html